https://doi.org/10.2352/ISSN.2470-1173.2017.14.HVEI-147

Measuring visually induced motion sickness using wearable devices

Ran Liu
Schepens Eye Research Institute, Massachusetts Eye and Ear, Department of Ophthalmology, Harvard Medical School, Boston, MA
College of Communication Engineering, Chongqing University, Chongqing 400044, China

Eli Peli and Alex D. Hwang
Schepens Eye Research Institute, Massachusetts Eye and Ear, Department of Ophthalmology, Harvard Medical School, Boston, MA

Abstract

Visually induced motion sickness (VIMS) is frequently reported with stereo and VR display systems. We tested whether VIMS can be detected by off-the-shelve wearable electrophysiology devices, where the VIMS were induced by driving in the virtual world. Our data indicates that 1) the correlation between blood pressure and heart rate, and 2) the changes of mean gravity frequencies in $TP9_{Delta}$ and $FP1_{Theta}$, and 3) the changes of SDs in $TP9_{Alpha}$ and $TP10_{Alpha}$ of the EEG signals may be possible candidates of the VIMS onset indicator. However, it is still hard to conclude that those physiological signals can be used as definitive VIMS indicators because our analysis only differentiates the physiological response to VIMS vs. non-VIMS, not the detection of VIMS onset, nor estimation of VIMS severity in real-time.

Introduction

Visually induced motion sickness (VIMS) is a discomfort disorder, which is often induced when a person is exposed to virtual and physical motions that are not well matched. For example, when a person immerses into a virtual environment of a driving simulator, the optic flow of the driving scene induces strong vection (self-motion illusion), but the vestibular system and the skeletomuscular system generates no self-motion because the person who drives is usually stationary in the static driver seat.

Mismatched motion signals are not limited to inter-sensory conflicts but may affect intra-sensory signal conflicts, such as dynamic spatiotemporal distortions of expected stability of rigid world [1].

A person experiencing VIMS suffers headaches, dizziness, disorientation, stomach awareness, nausea, and even vomiting. This phenomenon raises safety and health concerns with current virtual reality (VR) platforms, in particular, head mounted display (HMD) systems. The VIMS has been identified as a major hurdle to overcome for wider spread use of the VR systems. Although many VR HMDs incorporate motion trackers to synchronize the users' virtual view with physical motions, VIMS still occurs frequently, presumably because fully synchronized view is difficult to achieve.

Pre- and post- VIMS questionnaires [2] developed for flight simulators have been used as the main method to measure the presence and level of the VIMS experienced due to the virtual environment exposure. However, this subjective measure of the symptoms may strongly prime the subject, and only get coarse temporal changes of the VIMS. In other words, it generally measures aftereffects of the VIMS.

To investigate causes of the VIMS or develop a VIMS countermeasure, it is essential to have VIMS measuring methods that (objectively) quantify the magnitude of VIMS.

Physiological measures supporting the objective and frequent (quasi-continuous) measure, such as electrogastrography (EGG), electrocardiography (ECG), salivary cortisol level, blood pressure (BP), heart rate (HR), and electroencephalography (EEG) have been proposed and tested as possible objective markers of VIMS to overcome the limitations of the subjective VIMS rating.

Cheung et al. [3] reviewed more than 10 years of EGG studies connecting gastric activity with changes in VIMS level, and concluded that EGG was not a reliable measure for VIMS because the increase in gastric activity from 1cpm to 3cpm is not always presented in VIMS onset. However, Kim et al. [4] found that net tachygastria does increase with VIMS, and argue that the EGG can be used as a measure of the VIMS.

Ujike, et al. [5] computed the ratio of power between lower frequency (LF: 0.05-0.1 Hz) and high frequency (HF: 0.15-0.4 Hz) of the ECG, which is an index of sympathetic nerve activity, for 2D and 3D stimulus viewing groups, and they found an overall increase of LF/HF ratio in 3D compared to 2D, which matched well with the VIMS estimated by questionnaire. Similar results were reproduced by Kiryu, et al. [6].

Ramsey [7] measured heart rate (HR) and salivary cortisol level before and after exposing to virtual reality environment, and found an increase of both HR and cortisol level, and they correlate well with subjective VIMS questionnaire scores.

A study by Graybiel et al. [8] found that BP nor HR changes did not indicate VIMS level changes. However, Holmes et al. [9] reported that BP and HR variability are well correlated with the level of VIMS. The changes in BP and HR variability were also found by Yang, et al. [10], when subjects viewed 2D and S3D movies. Changes were larger for the 3D condition.

Sugita et al. [11] observed BP and HR changes during the VIMS stimulus exposure in VIMS-onset and non-VIMS-onset groups, and found that the temporal change of BP was less correlated to HR changes in VIMS onset group, suggesting that BP and HR correlation may be used as an objective VIMS measure. A similar conclusion was derived by Abe et al. [12] by computing the maximum cross-correlation coefficient between BP and HR variability using a finger photoplethysmography (PPG).

Electroencephalograph (EEG) was also tested as a surrogate measure of VIMS by Lin, et al. [13], Chen, et al. [14], and Naqvi, et al. [15]. All suggested that the alpha and gamma bands of the EEG power spectrum are valid indicators of VIMS, where a decrease in alpha band power represents a VIMS onset signature.

A recent fMRI study done by Miyazaki [16] suggested that asynchronous bilateral MT+ activation may be a marker of VIMS.

Although many studies have claimed that the VIMS can be measured by various autonomic responses, the large inter-subject variability and lack of repeatability suggest that no particular physiological measure (or combinations of measures) can be considered as reliable as the subjective scoring. Also, many of the measurements proposed require expensive clinical/scientific tools and invasive application to the skin or scalp which require gels and adhesives.

In this study, we tested the feasibility of using off-the-shelve, inexpensive wearable wireless devices for measuring VIMS, which we induced by virtual driving in the driving simulator, a task that is known to induce severe VIMS [17].

Methods

Participants

Fifteen normally sighted subjects aged from 20 to 45 were recruited from the Schepens Eye Research Institute. All subjects voluntarily signed an informed consent form approved by the Institute Review Board before the experiments. Nine subjects (4 males) completed the studies and reported here. The others six subjects served in pilot experiments and calibration of the set up.

Measuring devices

The Muse (InteraXon Inc., Ontario Canada), a wearable device, was used to record EEG continually. This EEG headband was designed for monitoring brain activity during the meditation through four EEG channels, two electrodes are at the frontal lobe (FP1 & FP2) and the other two are at the temporal lobe (TP9 & TP10). The EEG data was sampled at 10 bits and at 220Hz. The accelerometers in the Muse sampled user head motion at 50Hz. The Muse was connected via Bluetooth to a laptop computer for logging.

BP and HR were measured by the iHealth wireless blood pressure wrist monitor (BP7), and iHealth wireless pulse oximeter (PO3) (iHealth Labs Inc., California, USA). Both were connected to the logger (usually smartphone) via Bluetooth. It takes about 40 seconds for the BP7 to obtain a single BP and HR reading (including inflation and deflation of cuff), so BP was sampled every minute. The PO3 was a small oximeter placed on a fingertip that measures perfusion index, SpO2 levels, and HR every second. It was used to record HR continuously.

Driving simulator for inducing VIMS

Figure 1. A wide field VR environment driving simulator (FAAC Inc. Ann Arbor, MI) used to induce motion sickness.

We used a wide field (220°) driving simulator to induce VIMS (Fig. 1). Although the driving simulator is equipped with a motion seat and force feedback steering wheel, which provides proprioceptive motion stimulation matched with virtual motion, we have observed that about 30% of subjects participated in our previous driving simulator studies reported some level of VIMS.

Experimental procedure

In the pre-driving segment (Fig. 2), the subjects were seating at rest (for 1~3 minutes). Then the subjects were asked to maintain a quiet standing pose for one minute with eyes opened (labeled as "BO" for "Before-driving eye-Opened"), and eyes closed for another minute (labeled as "BC" for "Before-driving eye-Closed") to record the subjects' baseline physiological states. During these baseline measurements, subjects kept their left arm bent to heart level for BP and HR measurements.

After this baseline measurements, the subjects drove a long "winding road" in the simulator. Each subject had different motion sickness tolerance threshold so actual driving duration varied from several minutes to more than 30 minutes.

During the driving, the subjects were asked to verbally report their subjective rating of the VIMS level (VIMSL), which varies from 0 (non-VIMS), 1 (slight VIMS), 2 (moderate VIMS), 3 (severe VIMS), and 4 (very severe VIMS). The experimenters probed the subjects to report the VIMSL every minute, but also asked subject to report VIMSL when they felt a change in the discomfort level.

We used this simple asynchronous VIMSL reporting method, instead of using the lengthier VIMS questionnaires to obtain semi-continuous VIMS level the subjects experienced. Similar VIMS reporting scheme was successfully used by Fernandes, et al. [18] for measuring the effect of dynamic peripheral visual field restriction on VIMS.

The subjects continued to drive until they felt very uncomfortable. When the subjects reached their highest VIMSL that they could tolerate which could be less than the highest score, "4", the subjects stopped the driving. Some continued to drive for a couple of minutes after the first report of VIMSL of "4" while others quit right away after reporting a lower VIMSL.

Once the driving stopped, subjects got out of the driving simulator for post-driving measurements. The subject maintained a quiet standing pose for one minute with eyes opened (labeled as "AO" for "After-driving eye-Opened"), and another one minute with eyes closed (labeled for "AC" as "After-driving eye Closed"). Physiological data were recorded throughout the procedure.

In most of the cases (eight out of nine cases), we kept measuring the physiological data even after collecting the AC data while the subjects stood still until their VIMSL returned to zero. There were brief interruptions of measurements between eyes state changes (less than 10 seconds) and between segments (less than 1minutes).

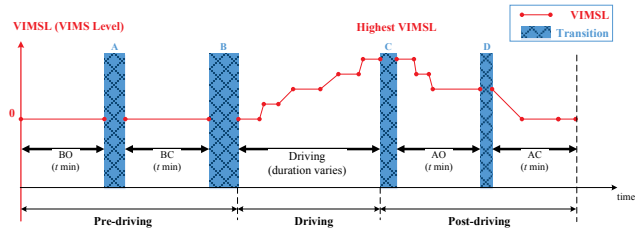

Figure 2. Timeline for experimental procedure and physiological measures, showing a schematic VIMS level changes for the corresponding segment.

Data processing

The purpose of our study was to determine whether specific physiological signal changes can be used as markers for a person's VIMS in VR environment. If there are such physiological measures, those measures should at least differentiate a person's physiological state between the VIMS and non-VIMS states.

In this study, we applied within subject comparisons for the mean and standard deviation (SD) of the physiological signals measured during the non-VIMS (baseline period: VIMSL=0) and VIMS (driving and recovering period: VIMSL>0) states to see if any physiological signal produces meaningful overall differences. The increase or decrease of the signal the means may represent a direct physiological response to the VIMS, while the physiological variation, SD, may indicate increase or decrease of disturbance in the physiological system due to VIMS.

For cardio data, the systolic (SYS) and diastolic (DIA) blood pressures were measured, and the pulse pressure (PP), a difference between SYS and DIA, was computed. The SD of each subject's measured blood pressures were normalized to their min and max values, making them varied from 0 to 1. The correlations between blood pressure measures (SYS, DIA, and PP) and HR in VIMS and non-VIMS stages were also computed.

For the EEG data, the power spectral density (PSD) functions for five frequency bands, delta (0-4 Hz), theta (4-8 Hz), alpha (8-12 Hz), beta (12-30 Hz) and gamma (30-50 Hz), were computed for the brain activity signals captured by each of the four electrodes for every one minute. Then the corresponding gravity frequencies (GF) within those frequency bands were computed. The differences between the signals on the left and right side of the brain were also computed for paired electrodes (TP10-TP9 and FP2-FP1) for each frequency band.

The GF of a PSD was defined as:

$$GF = \frac{\sum_{f1}^{f2} f \cdot \mathrm{PSD}(f)}{\sum_{f1}^{f2} \mathrm{PSD}(f)}, \qquad (1)$$

where f represents the frequency of the EEG signal, and f_1 and f_2 represent the lowest and highest frequency of a given frequency band.

Note that the PSD defines the energy distribution of a signal in the frequency domain for given time period, while the GF is a representative ("center of mass") frequency in a given frequency range, which conveys the same level of energy that the corresponding PSD carries. In other words, for a given frequency range, the energy carried by the signal in the frequency range lower than the GF is one-half of the total energy carried by the signal. Therefore, computing the GF for each PSD computation allows us to see the temporal changes in brain activity within a given frequency band.

Chen, *et al*. [19] argued that the GF can be used for measuring the visual fatigue. In their study, GFs of before and after watching the 60 minutes of S3D / 2D contents were computed and showed that watching S3D contents reduces the GF significantly more than watching 2D contents.

Results

Fig. 3a shows a subject's subjective VIMSL changes during the experiment. In this example, the increase of VIMSL started about 5 minutes after starting the driving (about 24 min), then started to decline a few minutes after stopping the driving.

Fig. 3b shows the time synchronized BP changes. A small increase of the SYS can be observed with the start of driving rather than VIMS onset, where the DIA showed no change during the driving. Both SYS and DIA values dropped with the end of driving. Fig. 3c shows the HR dropping with the start of driving then increases at the end of driving with no impact on the reported VIMS onset.

Fig. 3d-h shows the GF changes for each EEG channels in five different frequency bands. However, it is hard to visually detect any trend of changes correlated with either driving or VIMSL changes.

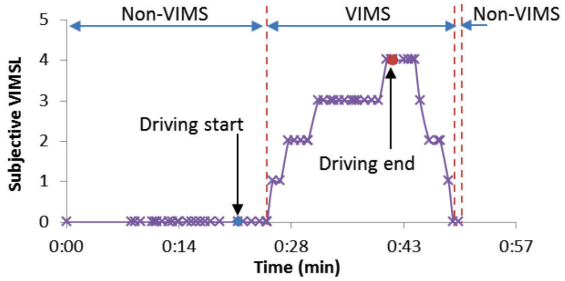

(a)

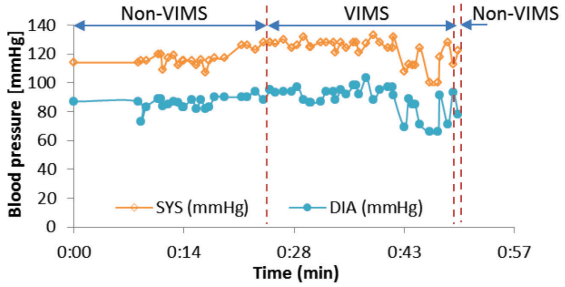

(b)

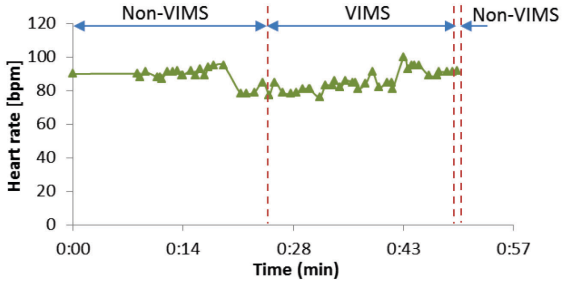

(c)

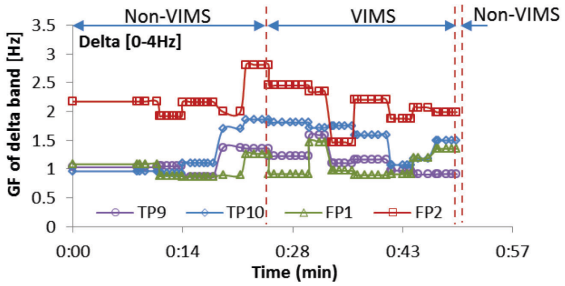

(d)

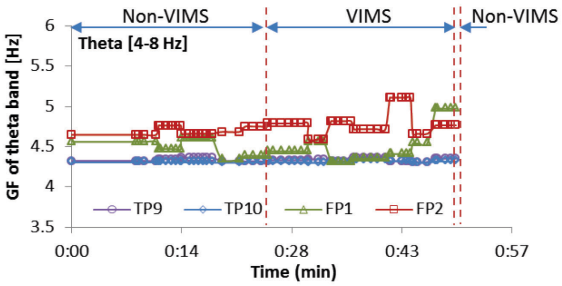

(e)

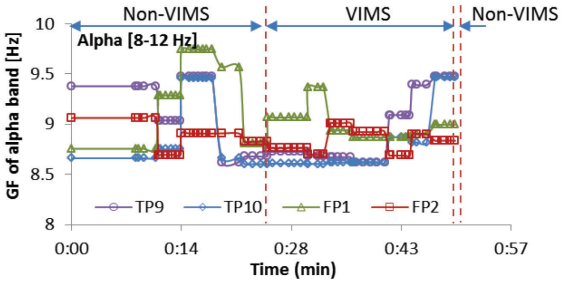

(f)

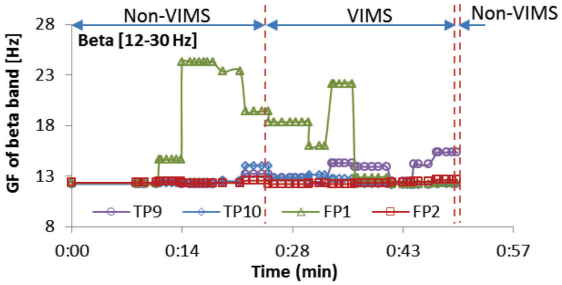

(g)

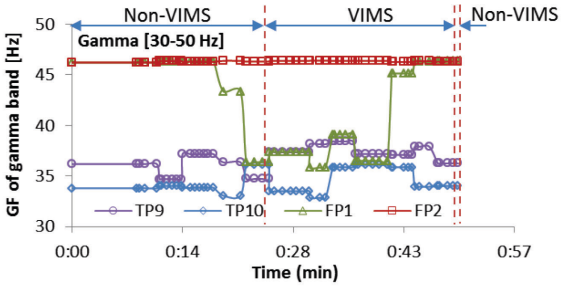

(h)

Figure 3. Time synchronized measurement results of a subject (S1), illustrating (a) VIMSL changes throughout the experiment, (b) blood pressure,(c) heart rate measured, and (d-h) GFs of the different EEG channels (TP9, TP10, FP1, and FP2) in five different frequency bands (delta, theta, alpha, beta, and gamma).

We computed the mean and SD of the nine subjects' SYS, DIA, PP, and HR measured in non-VIMS and VIMS sections. Fig. 4 shows the distribution of the measured data.

A pairwise t-test was applied to each physiological measure. The results (Fig. 4) show that there are no significant differences in all measurements. For the mean value: SYS ($t(8)=2.31$, $p=0.54$), DIA ($t(8)=2.31$, $p=1.0$), PP ($t(8)=2.31$, $p=0.66$, and HR ($t(8)=2.31$, $p=0.92$). For the SD: SYS ($t(8)=2.31$, $p=0.41$), DIA ($t(8)=2.31$, $p=0.06$), PP ($t(8)=2.31$, $p=0.08$, and HR ($t(8)=2.31$, $p=0.35$).

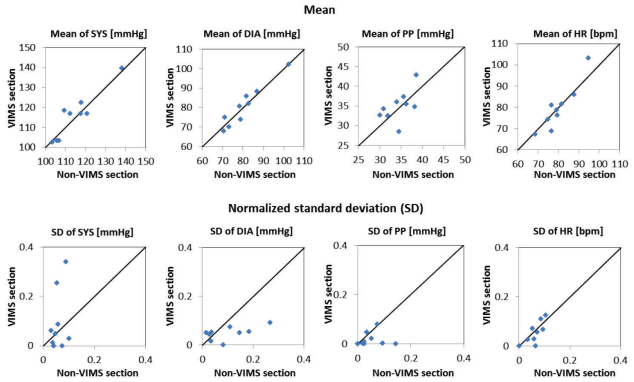

Figure 4. Comparison of the mean (top row) and standard deviation (bottom row) of systolic (SYS) and diastolic (DIA) blood pressure, pulse pressure (PP), and heart rate (HR) between non-VIMS and VIMS sections for each subject. Each dot in the plots represents a subject's data. If there is a significant trend of increase or decrease due to VIMS, the majority of dots should be located above or below the diagonal line, respectively. As shown above, in all comparisons, no significant difference between Non-VIMS and VIMS sections was found.

Also a pairwise *t*-test was applied to the correlations between 1) SYS and HR, 2) DIA and HR, 3) PP and HR in non-VIMS and VIMS sections, but all correlations were statistically insignificant: SYS-HR ($t(8)=2.31$, $p=0.70$), DIA-HR ($t(8)=2.31$, $p=0.78$), and PP-HR ($t(8)=2.31$, $p=0.60$).

However, it was observed that in non-VIMS section, 67% of subjects shows significant correlations ($r > 0.5$) in SYS-HR, but this correlation broke in VIMS section, where only 22% of subjects maintained significant correlation. Similar patterns of breaking down of the correlation were also found in DIA-HR (89%→44%) and PP-HR (56%→11%), as shown in Fig 5. This means that more subjects lost BP-HR correlation when the VIMS was onset.

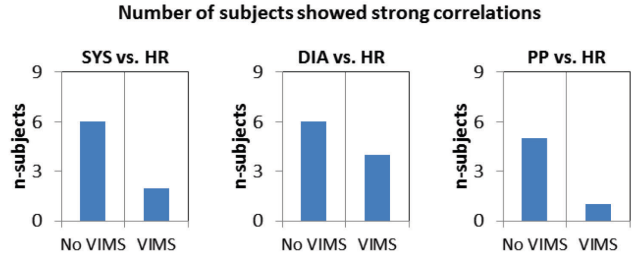

Figure 5. Number of subjects (out of 9 subjects) showed strong correlations between (a) SYS and HR, (b) DIA and HR, and (c) PP and HR in non-VIMS and VIMS sections. In all cases, the correlations between blood pressure and heart rate in non-VIMS sections are more likely to be 'significantly' correlated than those in VIMS sections. It may indicate that usual tendency of higher blood pressure associated with higher heart rate is more likely disturbed by VIMS.

Similar analyses were carried out for the EEG data based on computed GFs for each frequency band for all channels. Fig. 6 shows all GF measurements that resulted in statistically significant difference (all ts(8)=2.31, ps<0.05) between non-VIMS and VIMS sections. Significant differences were found for the mean values of $TP9_{Delta}$, $FP1_{Theta}$, and $TP10_{Beta}$, and SDs of $TP9_{Alpha}$ and $TP10_{Alpha}$.

In other channels and frequency bands, no significant difference between non-VIMS and VIMS sections was found (all ts(8)=2.31, ps>0.05).

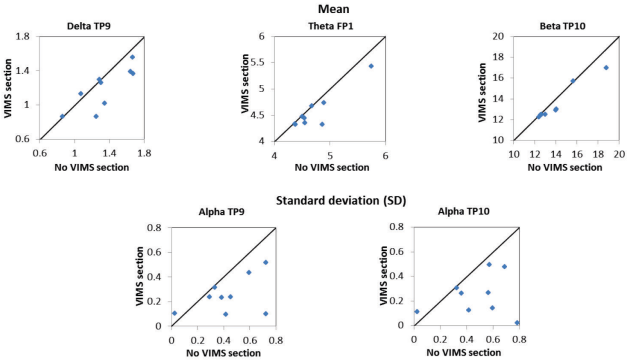

Figure 6. Comparison of the mean (top row) and standard deviation (bottom rows) of GFs for those frequency bands and channels that showed significant differences between non-VIMS and VIMS sections.

The correlations between left and right brain signal pairs (FP1-FP2 and TP9-TP10) for all frequency bands were also computed, then a pairwise t-test was applied to compare the mean correlations. For all frequency bands, no significant difference was found. Also, unlike the BP-HR correlation analysis, no particular trend of EEG signal correlation confidence level change was observed between non-VIMS and VIMS sections.

Using the off-the-shelf inexpensive wearable EEG devices, we have noted large signal variability (noise) in every band and channels from time to time. We suspect that those noisy data might be caused by the poor connection with the skin, so those data segments were excluded in our analysis (about 1.7% of total).

Results

This pilot study focused on the changes of the mean and standard deviation of various physiological signals in an attempt to detect VIMS occurrence in a VR environment.

Our data indicates that: 1) the mean and standard deviation changes of BP and PR may not be suitable for VIMS detection since they changed little between VIMS and non-VIMS state. 2) Reduction of correlation between BP (SYS, DIA, and PP) and HR may indicate the presence of VIMS. 3) For most of the channels and frequency bands of EEGs, the mean and SD of GF changes between VIMS and non-VIMS states are not significant, except the means in $TP9_{Delta}$ and $FP1_{Theta}$ and SDs in $TP9_{Alpha}$ and $TP10_{Alpha}$. 4) No significant change in the correlations between left and right brain signals (FP1-FP2 and TP9-TP10) were found for VIMS onset.

Although we found some significant differences between non-VIMS and VIMS states, it is still hard to conclude that these signals can be used as the VIMS indicators because our analyses, so far, only differentiate the physiological response to the VIMS over whole period including severe VIMS, not the detection of the VIMS onset, nor estimation of VIMS severity in real-time.

In order to confirm our findings, a repetition of these results is necessary. To make the finding useful, further analysis methods should be developed for timely detection and level estimation in real time.

Finally, since this study was conducted with the driving simulator, the elicitation of VIMS was a result of visual and physical interactions with the stimulus contents. Therefore, it may be difficult to determine if the measured physiological differences were caused by the emotional or physical impact of the task (e.g. driving) or solely reflects the impact of VIMS. Therefore, our results should be verified in a more controlled experimental design such as viewing the same video contents in different viewing methods, where one of the viewing methods is known to induce more VIMS (i.e., 2D vs. S3D).

Acknowledgements

Supported in part by Google Faculty Research Awards, and Chongqing foundation & advanced research project (cstc2016 jcyjA0103), and NIH grant R01EY024075. The authors declared that they have no financial interest to declare related to this work. Dr. Peli is a consultant to Google, and previously consulted to a number of other companies involved in HMD development that may be interested in VIMS in VR.

References

[1] Hwang, Alex D., and Eli Peli. "Instability of the perceived world while watching 3D stereoscopic imagery: A likely source of motion sickness symptoms." i-Perception 5, no. 6 (2014): 515-535.

[2] Kennedy, Robert S., Norman E. Lane, Kevin S. Berbaum, and Michael G. Lilienthal. "Simulator sickness questionnaire: An enhanced method for quantifying simulator sickness." The international journal of aviation psychology 3, no. 3 (1993): 203-220.

[3] Cheung, Bob, and Peter Vaitkus. "Perspectives of electrogastrography and motion sickness." Brain research bulletin 47, no. 5 (1998): 421-431.

[4] Kim, Young Youn, Eun Nam Kim, Min Jae Park, Kwang Suk Park, Hee Dong Ko, and Hyun Taek Kim. "The application of biosignal feedback for reducing cybersickness from exposure to a virtual environment." Presence: Teleoperators and Virtual Environments 17, no. 1 (2008): 1-16.

[5] Ujike, Hiroyasu, and Hiroshi Watanabe. "Effects of stereoscopic presentation on visually induced motion sickness." In IS&T/SPIE Electronic Imaging, pp. 786314-786314. International Society for Optics and Photonics, 2011.

[6] Kiryu, T. and Iijima, A., 2014, October. A multi-timescale autonomic regulation model for interpreting visually induced motion sickness. In 2014 IEEE 3rd Global Conference on Consumer Electronics (GCCE) (pp. 254-257). IEEE.

[7] Ramsey, A. D. "Changes in salivary cortisol, pulse rate and self-report during longer immersions in interactive virtual environments." The Journal of Psychosomatic Medicine (1997).

[8] Graybiel, A. and Lackner, J.R., 1980. Evaluation of the relationship between motion sickness symptomatology and blood pressure, pulse

rate, and body temperature. Aviation, space, and environmental medicine, 51(3), pp.211-214.

[9] Holmes, Sharon R., and Michael J. Griffin. "Correlation between pulse rate and the severity of motion sickness caused by optokinetic stimulation." Journal of Psychophysiology 15, no. 1 (2001): 35.

[10] Yang, Xinpan, Danli Wang, Haichen Hu, and Kang Yue. "P-31: Visual Fatigue Assessment and Modeling Based on ECG and EOG Caused by 2D and 3D Displays." In SID Symposium Digest of Technical Papers, vol. 47, no. 1, pp. 1237-1240. 2016..

[11] Sugita, Norihiro, Makoto Yoshizawa, Akira Tanaka, Kenichi Abe, Shigeru Chiba, Tomoyuki Yambe, and Shin-ichi Nitta. "Quantitative evaluation of effects of visually-induced motion sickness based on causal coherence functions between blood pressure and pulse rate." Displays 29, no. 2 (2008): 167-175.

[12] Abe, Makoto, Makoto Yoshizawa, Norihiro Sugita, Akira Tanaka, Shigeru Chiba, Tomoyuki Yambe, and Shin-ichi Nitta. "A method for evaluating effects of visually-induced motion sickness using ICA for photoplethysmography." In 2008 30th Annual International Conference of the IEEE Engineering in Medicine and Biology Society, pp. 4591-4594. IEEE, 2008.

[13] Lin, Chin-Teng, Shu-Fang Tsai, Hua-Chin Lee, Hui-Lin Huang, Shinn-Ying Ho, and Li-Wei Ko. "Motion sickness estimation system." In The 2012 International Joint Conference on Neural Networks (IJCNN), pp. 1-6. IEEE, 2012.

[14] Chen, Yu-Chieh, Jeng-Ren Duann, Shang-Wen Chuang, Chun-Ling Lin, Li-Wei Ko, Tzyy-Ping Jung, and Chin-Teng Lin. "Spatial and temporal EEG dynamics of motion sickness." NeuroImage 49, no. 3 (2010): 2862-2870.

[15] Naqvi, Syed Ali Arsalan, Nasreen Badruddin, Munsif Ali Jatoi, Aamir Saeed Malik, Wan Hazabbah, and Baharudin Abdullah. "EEG based time and frequency dynamics analysis of visually induced motion sickness (VIMS)." Australasian Physical & Engineering Sciences in Medicine 38, no. 4 (2015): 721-729.

[16] Miyazaki, J., Yamamoto, H., Ichimura, Y., Yamashiro, H., Murase, T., Yamamoto, T., Umeda, M. and Higuchi, T., 2015. Inter-hemispheric desynchronization of the human MT+ during visually induced motion sickness. Experimental brain research, 233(8), pp.2421-2431.

[17] Classen, Sherrilene, Megan Bewernitz, and Orit Shechtman. "Driving simulator sickness: an evidence-based review of the literature." American journal of occupational therapy 65, no. 2 (2011): 179-188.

[18] Fernandes, Ajoy S., and Steven K. Feiner. "Combating VR sickness through subtle dynamic field-of-view modification." In 2016 IEEE Symposium on 3D User Interfaces (3DUI), pp. 201-210. IEEE, 2016.

[19] Chen, C., Wang, J., Li, K., Wu, Q., Wang, H., Qian, Z. and Gu, N., 2014. Assessment visual fatigue of watching 3DTV using EEG power spectral parameters. Displays, 35(5), pp.266-272.

Author Biography

Ran Liu *received his B.E., M.E. and D.E. degrees in computer science from Chongqing University, Chongqing, China in 2001, 2004 and 2007, respectively. He worked as a postdoctoral researcher in Homwee Technology Co., Ltd., Chengdu, China, from 2008 to 2010. He is an associate professor in the College of Communication Engineering, Chongqing University. He is also a visiting scholar in Schepens Eye Research Institute. His research interests include stereo vision and computer vision.*

Eli Peli *received BSc and MSc in electrical engineering from Technician-Israel Institute of Technology (IIT), Haifa, Israel (1979), and OD from New England College of Optometry, Boston, MA (1983). Since then he has been at the Schepens Eye Research Institute where he is a Senior Scientist and the Moakley Scholar in Aging Eye Research, and Professor of Ophthalmology at Harvard Medical School.*

Alex D. Hwang *received BS in mechanical engineering from the University of Colorado Boulder (1999), and received MS (2003) and Ph.D. in computer science from the University of Massachusetts Boston (2010). Since then, he has worked at Schepens Eye Research Institute in Boston MA as a postdoctoral fellow. He became an Investigator and is appointed as an Instructor of Ophthalmology at Harvard Medical School (2015). His work has focused on bioengineering and low vision rehabilitation.*